Atmospheric Research 242 (2020) 104983

Contents lists available at ScienceDirect

Atmospheric Research

journal homepage: www.elsevier.com/locate/atmosres

Diagnosis of a high-impact secondary cyclone during HyMeX-SOP1 IOP18

D.S. Carrió[a,b,*], V. Homar[a], A. Jansà[a], M.A. Picornell[c], J. Campins[c]

[a] Meteorology Group, Department of Physics, Universitat de les Illes Balears, Palma de Mallorca, Spain
[b] School of Earth Sciences and ARC Centre of Excellence for Climate Extremes, The University of Melbourne, Victoria, Australia
[c] Agencia Estatal de Meteorología, Palma de Mallorca, Spain

ARTICLE INFO

Keywords:
Secondary cyclone
High-impact event
Factor separation
Potential vorticity inversion
Mediterranean
HyMeX

ABSTRACT

Multiple high-impact weather events occurred during HyMeX-SOP1, which was intensively monitored by a large number of ordinary and extraordinary observations. The availability of special observations offers an unprecedented opportunity to explore these events in depth and assess the capabilities of current numerical weather prediction tools. In this case, a small-scale secondary cyclone formed within a prominent cyclone that intensified in the north-western part of the western Mediterranean during IOP18 on October 31, 2012. The small secondary system formed near Catalonia, where heavy rain was observed, and then moved to the northern part of the island of Minorca, producing very strong winds. Finally, the secondary cyclone moved northeast while merging with the main cyclone and evolving as a cyclonic perturbation towards the Gulf of Genoa, bringing heavy precipitation to some Italian regions.

This work aims at providing a detailed diagnosis of the genesis and evolution of the secondary cyclone, using high-resolution numerical tools. Furthermore, with the main objective of identifying the main physical mechanisms involved in the genesis and evolution of the small-scale secondary cyclone, sensitivity experiments were performed taking into account three main factors: latent heat release, upper-level dynamical forcing and topographical effects. Results show that in terms of individual cyclogenetic contributions, the upper level PV anomaly contribution dominated the initial phase and the diabatic heating from condensation contributed to the further deepening during the later stages of the secondary cyclone. The initial dynamical effect from the upper-levels forcing was amplified by the local topographic features, becoming a key synergistic factor for the formation of the damaging secondary cyclonic system.

1. Introduction

The Hydrological Cycle in the Mediterranean Experiment (HyMeX) is a decade-long international program (2010–2020) that aims at advancing the scientific knowledge of the Mediterranean water cycle variability, and improving our understanding of physical models, as well as regional climate models, with an emphasis on hydro-meteorological extremes (Drobinski et al., 2014). The HyMeX observation strategy is based on three-level nested observation periods: long-term (LOP), enhanced (EOP), and special (SOP) observation periods. The first SOP, HyMeX-SOP1, was a field campaign focusing on heavy precipitation and flash flooding, which was carried out during fall 2012 (September 5–November 6), over the north-western Mediterranean target area (Ducrocq et al., 2014). During SOP1, some intensive observation periods (IOPs) were defined. In most of the six IOPs that affected Spanish regions, a low-level cyclone could be identified, contributing to heavy rain and flooding (Jansà et al., 2014). Specifically, Flaounas et al. (2016) and Mariani et al. (2015) analysed IOP16 and IOP18, which were triggered by two deep cyclones that produced torrential rainfall in northeast Spain and northwest Italy.

For the case of IOP18, the AROME-WMED reanalysis (Fourrié and Nuret, 2014) performed using operational and additional data- shows a deep cyclone over the north-western Mediterranean, which intensified near Catalonia and progressed towards the Gulf of Genoa producing strong winds and heavy precipitation in some regions of Spain and Italy. This reanalysis also reveals an interesting small-scale evolution: a few hours after the precipitation peak in Catalonia, an intense small-scale secondary cyclone was formed in the region. This intense secondary cyclone moved towards the north of Minorca while very strong sudden winds affected the island. Although the main deep low-pressure system of the IOP18 event was previously analysed (e.g., Flaounas et al. (2016) and Mariani et al. (2015)), no diagnose study was performed

* Corresponding author at: School of Earth Sciences and ARC Centre of Excellence for Climate Extremes, The University of Melbourne, Parkville 3010, Victoria, Australia.
E-mail address: diego.carriocarrio@unimelb.edu.au (D.S. Carrió).

https://doi.org/10.1016/j.atmosres.2020.104983
Received 19 August 2019; Received in revised form 5 March 2020; Accepted 2 April 2020
Available online 08 April 2020
0169-8095/

referring to the initiation and posterior evolution of this small but intense secondary cyclone, which strongly impacted Minorca Island.

As grid resolutions increase, numerical models can represent and describe smaller scales and particularly smaller cyclonic structures. Most of these cyclones do not produce relevant weather, but some produce strong winds and heavy rain events. A clear case of this relatively rare type of Mediterranean cyclone, known as medicane (**Medi**terranean Hurri**cane**; Emanuel, 2005), has received special attention from the community over the last two decades: Lagouvardos et al., 1999; Homar et al., 2003; Fita et al., 2007; Buzzi, 2010 or Tous and Romero (2013). Notwithstanding the advances in understanding the processes and mechanisms leading to the genesis and intensification of medicanes, the scientific community has not yet reached a common agreement for the definition of a medicane.

The large availability of data for HyMeX-SOP1 allowed the generation of a reliable high resolution reanalysis (AROME-WMED) and thus provides the opportunity for studying a substructure that is important to comprehensively investigate the impacts of this damaging cyclone. Such secondary cyclones do not get as much attention as medicanes, but constitute another proof of the wide diversity of Mediterranean cyclones, especially in the small-scales. Note that, despite current numerical weather models provide valuable information about the genesis and evolution of medicanes (e.g., Davolio et al., 2009; Carrió et al., 2017; Pytharoulis, 2018, accurate short-range numerical predictions of this secondary cyclonic structures still represent an important forecasting challenge.

The main scope of this study is to contribute to the current understanding of Mediterranean cyclones, focusing specially on the quick formation of cyclonic substructures within them. Essentially, the concrete aim of this study is twofold: i) to analyse the link between the secondary structure formed within the prominent cyclone, present over the western Mediterranean on 31 October 2012, and the sudden extreme winds that affected Minorca that day, and ii) to explore and understand the physical mechanisms that contributed to the development of the secondary cyclone. To achieve both goals we first present a description of the event from an observational point of view. Later, the evolution of the main and secondary low centres is examined from the WMED reanalysis, by using the objective detection procedure described in Picornell et al. (2001) and Campins et al. (2006), which has been significantly improved to accurately describe small-scale cyclones (Picornell et al. 2013). Finally, sensitivity and attribution techniques, such as the factor separation technique of Stein and Alpert (1993) provide a clear depiction of the cyclogenetic mechanisms acting during the life cycle of both cyclones.

2. Synoptic and mesoscale analysis

2.1. Relevant observations

On October 31, 2012, the western Mediterranean was affected by a high-impact weather event. Up to 112 mm of precipitation were recorded over 12 h in Catalonia and 60 mm in the Balearic Islands, while strong winds affected Minorca and Sardinia (and the rest of the Balearic Islands, but to a lesser extent). During 30 and 31 October, a cut-off low aloft, was progressing eastward across the Iberian Peninsula overlapping a pre-existing low mean sea level pressure (MSLP) area over the western Mediterranean. The air mass images show a spiral cloud mass associated with the regenerated, intensified multilevel low, moving eastward (Fig. 1). At 0900 UTC, a dry slot between the frontal cloud band and the cloud head can be clearly observed (Fig. 1b); it is presumably linked to a dry air intrusion and was curling during the subsequent hours (Fig. 1d-f). At mid-levels, a cloud band, extending from Algeria to the northern Balearic Islands, which formed along the northern boundary of a warm air advection area extending from the south, is clearly identifiable at 0600 UTC (Fig. 1a). Initially, the low-level cyclonic disturbance was small in size and not very intense, but a warm south-eastern inflow from the Mediterranean Sea towards Catalonia provided warm moist air that fed precipitation systems active in the area. Heavy rain was recorded along the north-western Mediterranean coastlands. Later, this cyclone intensified progressively and overall, frontal cloud bands compare well with the inflow of cold and warm conveyor belts of the cyclone (compare Fig. 1 with Fig. 5c from Flaounas et al. (2016)).

At 1230 UTC a MSLP of 987 hPa, intense precipitation, and very strong westerly winds ($20\,m\,s^{-1}$ sustained speed, with gusts of $32.5\,m\,s^{-1}$) were reported by the weather station at the airport in Minorca (Fig. 2) and several flights were delayed or rerouted. Historical records show that these observations are rare, with only 13 and 7 cases of lower MSLP and higher wind gusts in 40 years at this station (Jansà et al., 2014). On the other hand, and linked to the main cyclone circulation, winds above $20\,m\,s^{-1}$ were recorded at buoys in the Gulf of Lions and Cote d'Azur, with significant wave heights exceeding 6 and 4 m, respectively. Finally, around 2100 UTC, strong winds were also recorded in Sardinia.

2.2. Numerical diagnosis

The spatial and temporal evolution of small scale aspects of this event are diagnosed using the AROME-WMED reanalysis (hereafter WME). The WME is a reanalysis adaptation of the AROME-WMED model, a real-time mesoscale model covering the western Mediterranean basin, that was set-up for the HyMeX SOPs and is based on the operational AROME-FRANCE, a convection-permitting model with a horizontal resolution of 2.5 km and 60 vertical levels. Additional observations collected during the SOPs were assimilated into the WME to improve the reanalysis (Fourrié and Nuret, 2014).

Besides official definitions at national level -mostly devoted to set objective criteria for legal or administrative processes-, there is no physically-based objective definition of cyclone (Neu et al., 2013). Indeed, the number and type of cyclones -or cyclonic structures- that can be detected and tracked depend heavily on the algorithm and resolved scales of the data used. Here, we use an adapted version of the Picornell et al. (2014) detection and tracking algorithm to identify and characterize the cyclones in the WME analysis. The adaptation consists in a weaker smoothing of MSLP fields and the tuning of selection criteria to preserve the main features of the small-scale cyclones, even secondary systems, formerly considered noise. This methodology is required when applied to kilometric resolutions and allows to detect and track small-scale cyclones, even secondary systems.

On October 31 at 0000 UTC, a cyclone was detected to the southwest of the Balearic Islands, which progressively moved towards the northeast, while deepening and organizing a more intense cyclonic circulation with time (Fig. 3). During the intensification phase (from 0000 UTC to 1500 UTC), the central MSLP of this cyclone dropped at a rate of $0.7\,hPa\,h^{-1}$, which is close to the $0.8\,hPa\,h^{-1}$ value set by Sanders and Gyakum (1980) to qualify as explosive cyclogenesis. We will refer this cyclone as the main or principal cyclone (hereafter PC). At 0600 UTC, a new, small secondary cyclonic centre (hereafter SC) was also identified by the detection algorithm off the Catalan coast (Fig. 4a). Along the subsequent hours, the SC moved slowly east-southeastwards over the sea (Fig. 3), following the movement of the main heavy rain area. The SC was detected with the MSLP minimum but could also be identified as a small and intense geostrophic vorticity maximum. At 1200 UTC, the SC became an open low, or convergence zone, located just offshore the northeast part of Minorca Island (westernmost empty blue square marker in Fig. 3). At that time (Fig. 4c), the central MSLP was 988.8 hPa, close to the 987.0 hPa observed at the Minorca airport, and with a strong MSLP gradient at low levels, which is consistent with the strong westerly winds that were also being recorded. During the following hours (Fig. 4d-4f), the SC merged with the PC, and progressed eastwards as a secondary perturbation, with intense pressure gradients that produced very strong westerly winds over Sardinia.

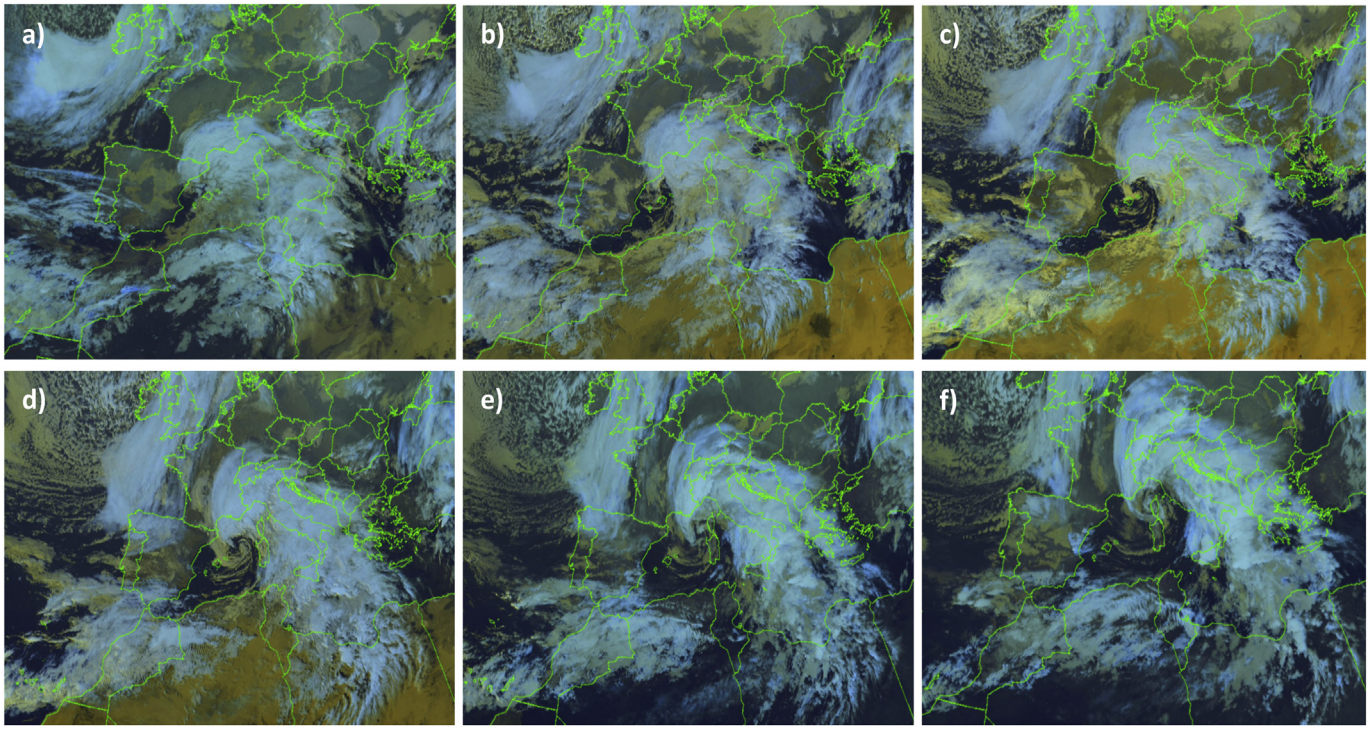

Fig. 1. Air mass RGB composite images from Meteosat Second Generation at 0600, 0900, 1200, 1500, 1800 and 21 UTC (a-f respectively).

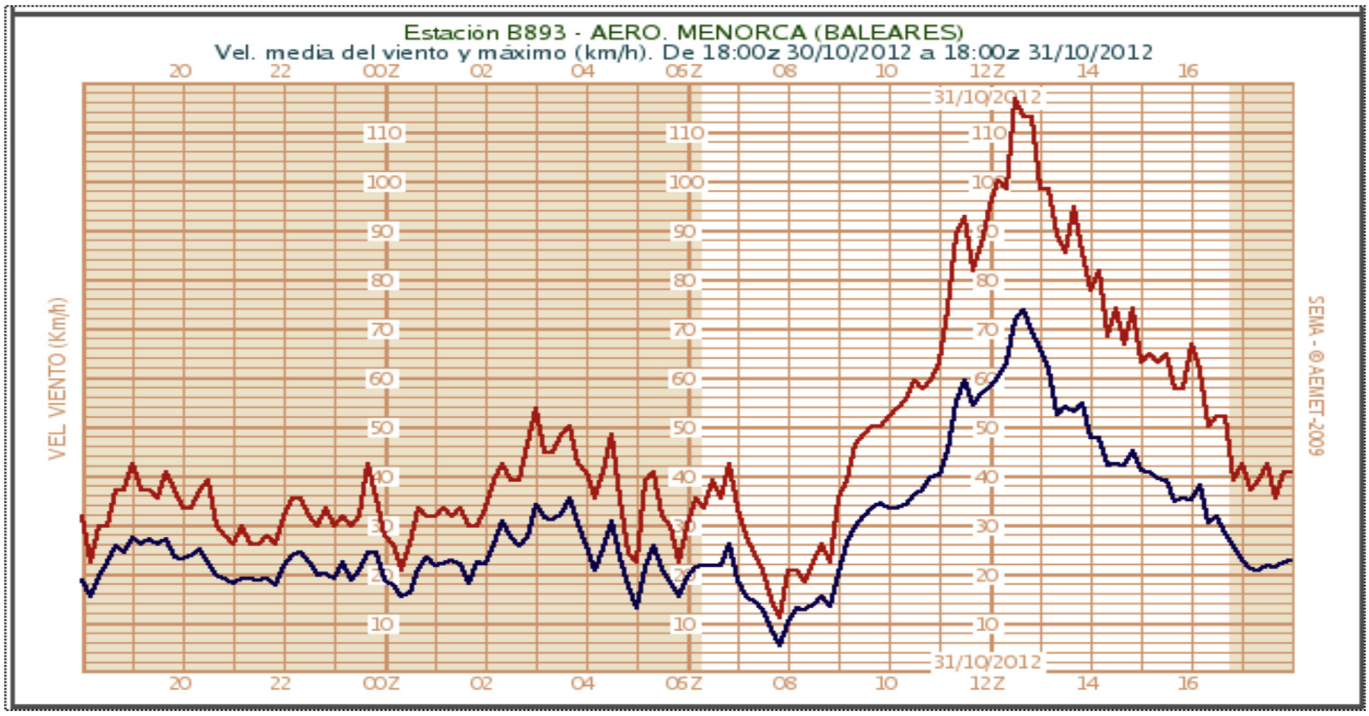

Fig. 2. Time series of wind gusts (red line) and sustained wind (black line) registered at the Airport of Minorca from 18 UTC 30 October to 18 UTC 31 October 2012. (For interpretation of the references to colour in this figure legend, the reader is referred to the web version of this article.)

3. Control run

A detailed diagnosis of this event is performed by means of a set of high-resolution numerical sensitivity experiments. These experiments allow to identify the key forcings of the intense cyclogenesis observed over the western Mediterranean and to attribute the associated strong winds that impacted Minorca. The significance of numerical sensitivity experiments results is conditioned to the existence of a sufficiently accurate control simulation that reproduces the relevant observed aspects of the event. Following is a description of the numerical configuration and a brief description of the control simulation results.

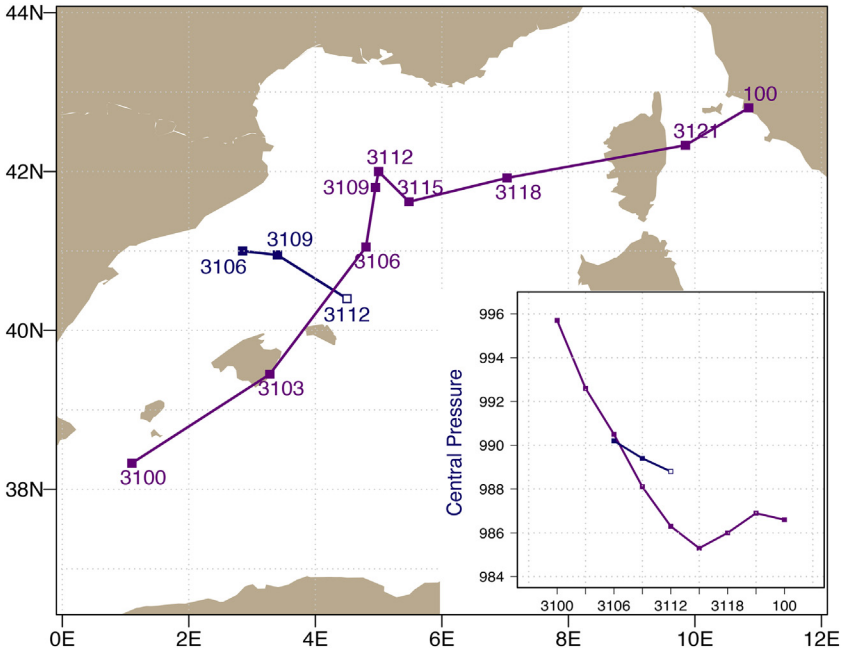

Fig. 3. Analysed primary (purple solid line) and secondary cyclone (blue solid line) tracks from WME during 31 October 2012. The embedded figure depicts the MSLP value evolution in the centre of PC (purple line) and the SC (blue line) from WME. (For interpretation of the references to colour in this figure legend, the reader is referred to the web version of this article.)

3.1. Model set-up

The Advanced Research Weather Research and Forecasting Model (WRF-ARW v3.4; Skamarock et al., 2008) is employed in this study; it is a non-hydrostatic mesoscale model that solves the primitive Euler equations system in flux form using terrain-following eta (η) coordinates. Initial and boundary conditions are obtained every six hours from the European Centre for Medium-Range Weather Forecasts (ECMWF). The numerical setup consists of a one-way nesting domain configuration centred in the western Mediterranean region (Fig. 5) with a parent domain at a 16-km horizontal grid resolution (423x241x51 grid points) and a high-resolution nested domain at a 2.5-km grid resolution (361x361x51 grid points) centred over the Balearic Islands. The η vertical levels are spaced less than 100 *m* apart near the surface to over 1 km apart at model top. With the main objective of avoiding spin-up model imbalances on the simulation of the event, the runs are initiated 12 h before the small intense cyclone hit Minorca, i.e., using the October 31, 00 UTC ECMWF operational analysis as initial conditions.

The specific physical parameterization options employed in the control simulation include: the single-moment Thompson microphysics scheme (Thompson et al., 2004, 2008), the short- and long-wave (SW/LW) radiation scheme RRTMG (Iacono et al., 2008), and the non-local Yonsei University (YSU) planetary boundary layer scheme (Hong et al., 2006) which uses an explicit entrainment layer and a parabolic K profile in an unstable mixed layer. The Kain-Fritsch scheme (Kain and Fritsch, 1993; Kain, 2004) is used on the parent domain to account for sub-grid convective effects. No convective parametrization is activated in the 2.5 km grid resolution nested domain.

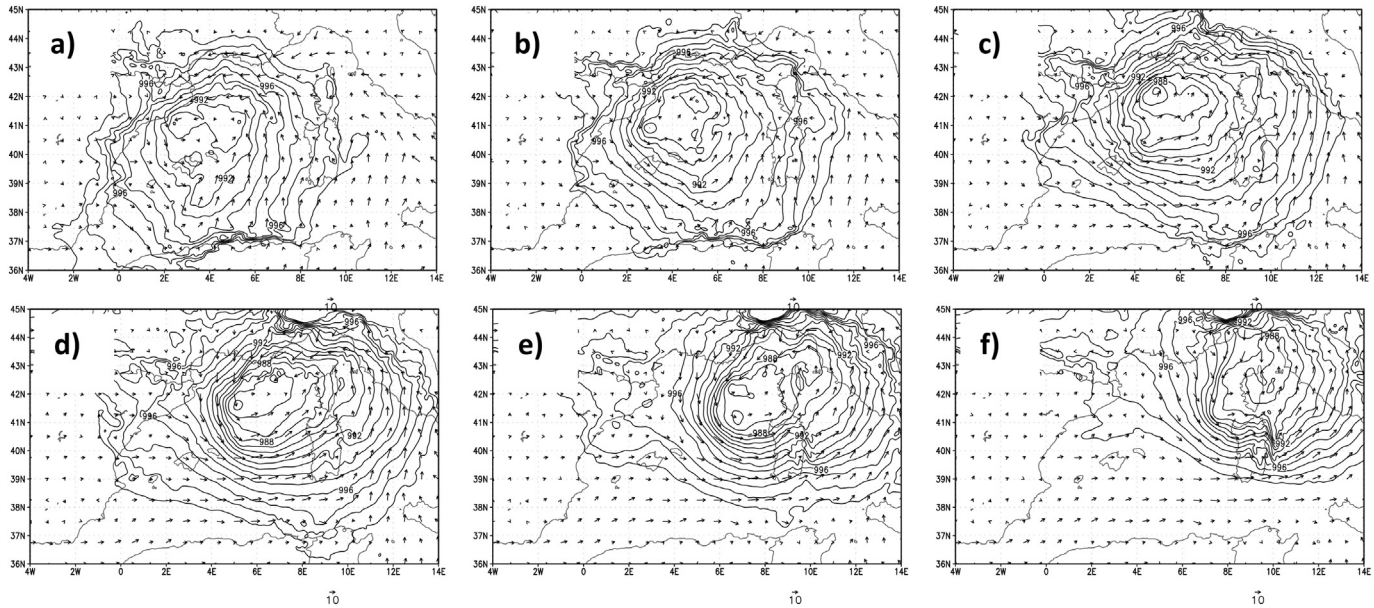

Fig. 4. MSLP (pressure < 1000 hPa countering interval Dp = 1 hPa, in black) and surface wind at 10 *m* AGL from WME October 31 at 06, 09, 12, 15, 18 and 21 UTC (a-f respectively).

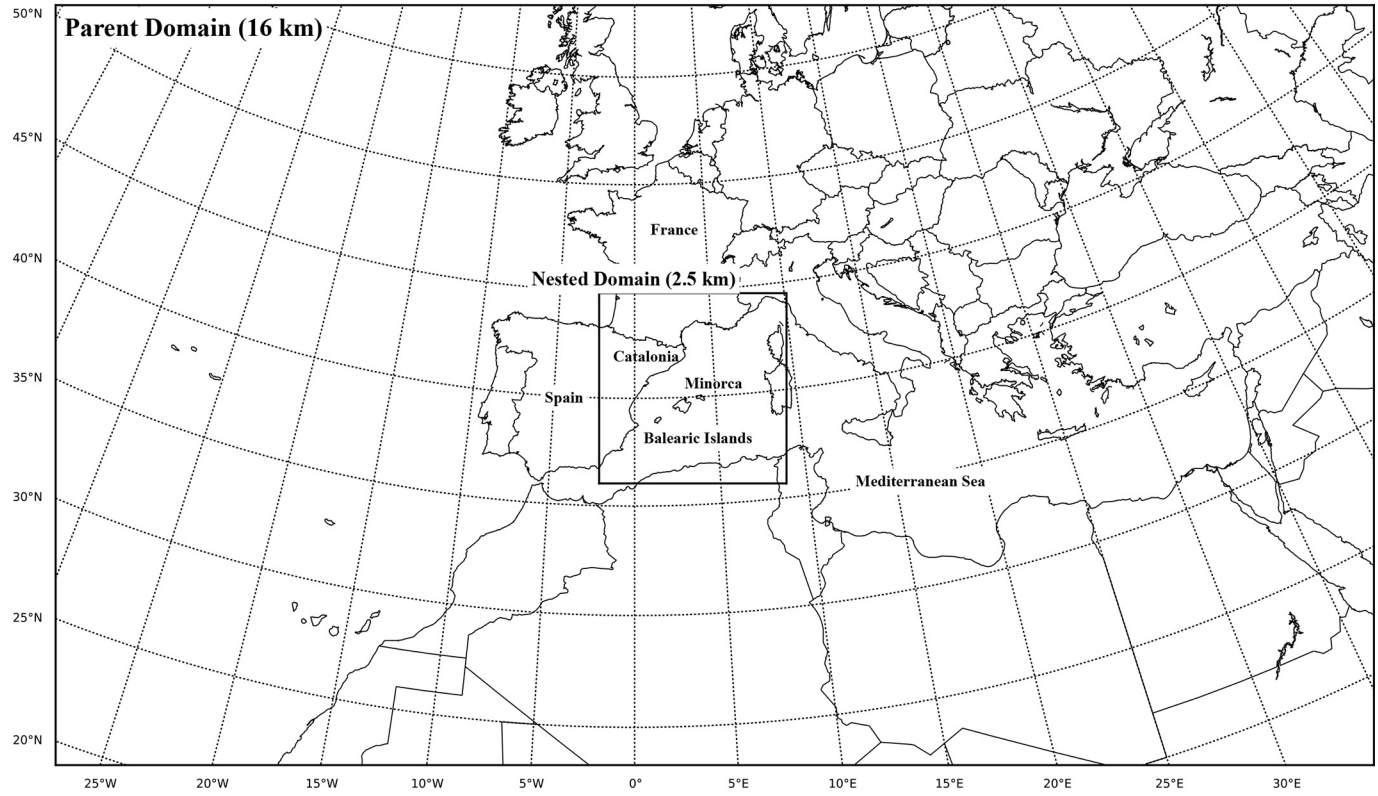

Fig. 5. Numerical domain configuration centred over the Western Mediterranean basin used to perform the entire set of numerical experiments in this study.

3.2. Verification of the control run

A verification of the control run is performed to determine its value in further numerical sensitivity experiments.

First, we compare the evolution of the MSLP—recorded at the Minorca airport—to the simulated values (CNTRL) at the closest grid point to Minorca (Fig. 6). During the first 6–7 h of 31 October, the simulated MSLP and the observations are linearly decreasing, from nearly 998 hPa to 989 hPa, with similar rates and values. The MSLP reduction observed during this period of time is mainly related with the evolution and intensification of PC, which is moving towards the northeast of the Balearic Islands. However, from 0600 to 1300 UTC the simulated MSLP values slightly depart from observations in Minorca by 1–2 hPa. Even with this minor discrepancy, the model satisfactorily simulates the genesis, intensification and evolution of the SC. After 1300 UTC, CNTRL accurately simulate observed MSLP values in Minorca. During this phase, the SC dissipates within the main cyclone and the MSLP recorded at Minorca airport is driven mainly by the PC influence alone. Therefore, results show that CNTRL accurately verifies observations during October 31, within a 1–2 hPa error range, and satisfactorily captures the deepening phase and the minimum MSLP value of nearly 987 hPa around 1200 UTC at the Minorca airport surface station.

Similarly, and taking into account that the wind that affected Minorca was extreme, 10 m winds recorded at the Minorca airport are also used to verify the control run (Fig. 7). Encouragingly, maximum simulated winds pick at the same time than observed values, with a reported maximum of 19.4 $m\,s^{-1}$ at 1300 UTC. It is important to note that winds in Minorca Airport from 1100 UTC to 1500 UTC are associated primarily to the SC, and both model and observations show similar evolutions. However, winds are in general overestimated by CNTRL. This positive bias could be originated by an error in the SC intensity, in its trajectory or both. In fact, these overestimated wind values could be explained as a result of a persistent southwest trajectory shift performed by CNTRL, in comparison with WME, that was found during the first 6 h of the lifespan of SC (Fig. 8). Such trajectory shift results in a simulated SC closer to the airport of Minorca, producing locally stronger winds than the WME.

The control run is also analysed in terms of its accuracy in simulating the principal cyclone. Simulated precipitable water (PW), integrated between 650 and 200 hPa, is used as a pseudo-satellite product:

$$PW = g^{-1} \int_{P650}^{P200} q dp,$$

where q is the specific humidity and g is the gravity acceleration. This product is directly compared to water vapour content derived from Meteosat-Seviri EUMETSAT instruments (6.2 μm) which is representative of the upper levels between 650 and 200 hPa (Fig. 9). Simulated PW shows, in agreement with the SEVIRI images, a clear intrusion of dry upper air curling around the low-pressure centre of the main cyclone from 0900 to 1500 UTC on October 31.

The abovementioned precision of CNTRL to simulate the synoptic and mesoscale features of the primary and secondary cyclones, authorizes the use of numerical sensitivity techniques to derive reliable and dependable conclusions about key mechanisms affecting the genesis and evolution of the cyclones with high level of confidence.

4. Cyclogenetic mechanisms of the secondary cyclone

Hypothetically, both dynamical and thermodynamical factors contributed to the genesis of the secondary cyclone. In terms of dynamics, a persistent eastern maritime flow, associated with the primary cyclone, is simulated during the first hours of the day. This moist flow impinged on the Catalan coast (Fig. 10a) and the prominent topography in the area acted as a geographical wind barrier, inducing a low-level convergence zone that favoured the triggering of deep convection (see red circle in Fig. 10 (a-c)). As a result, efficient condensation occurred, releasing significant amounts of latent heat, and also producing intense precipitation (Fig. 10 (d-f)). The diabatic warming associated with this

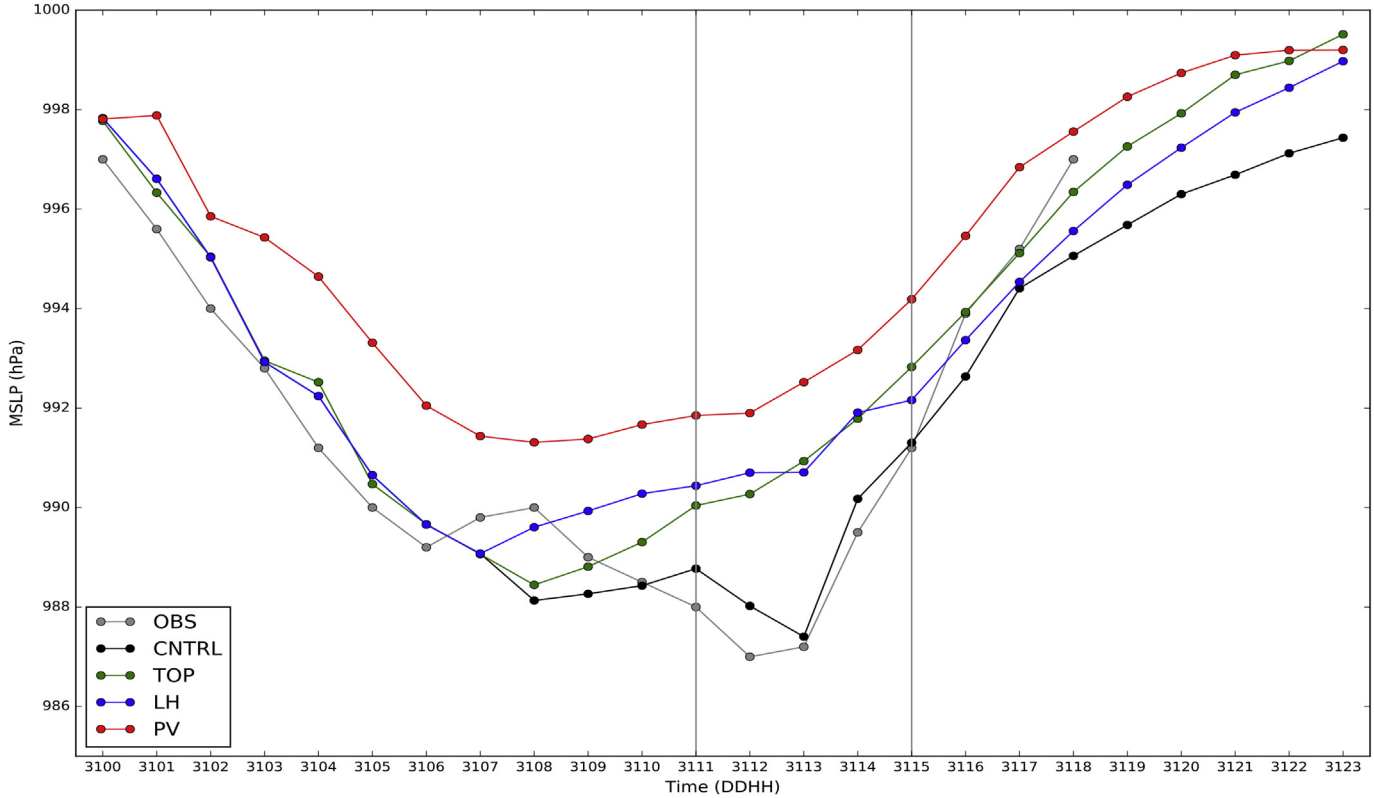

Fig. 6. MSLP observed (solid grey line) and simulated (solid color lines) by the different numerical experiments performed in this study between 00–23 UTC on 31 October 2012 at the closest point to the airport of Menorca.

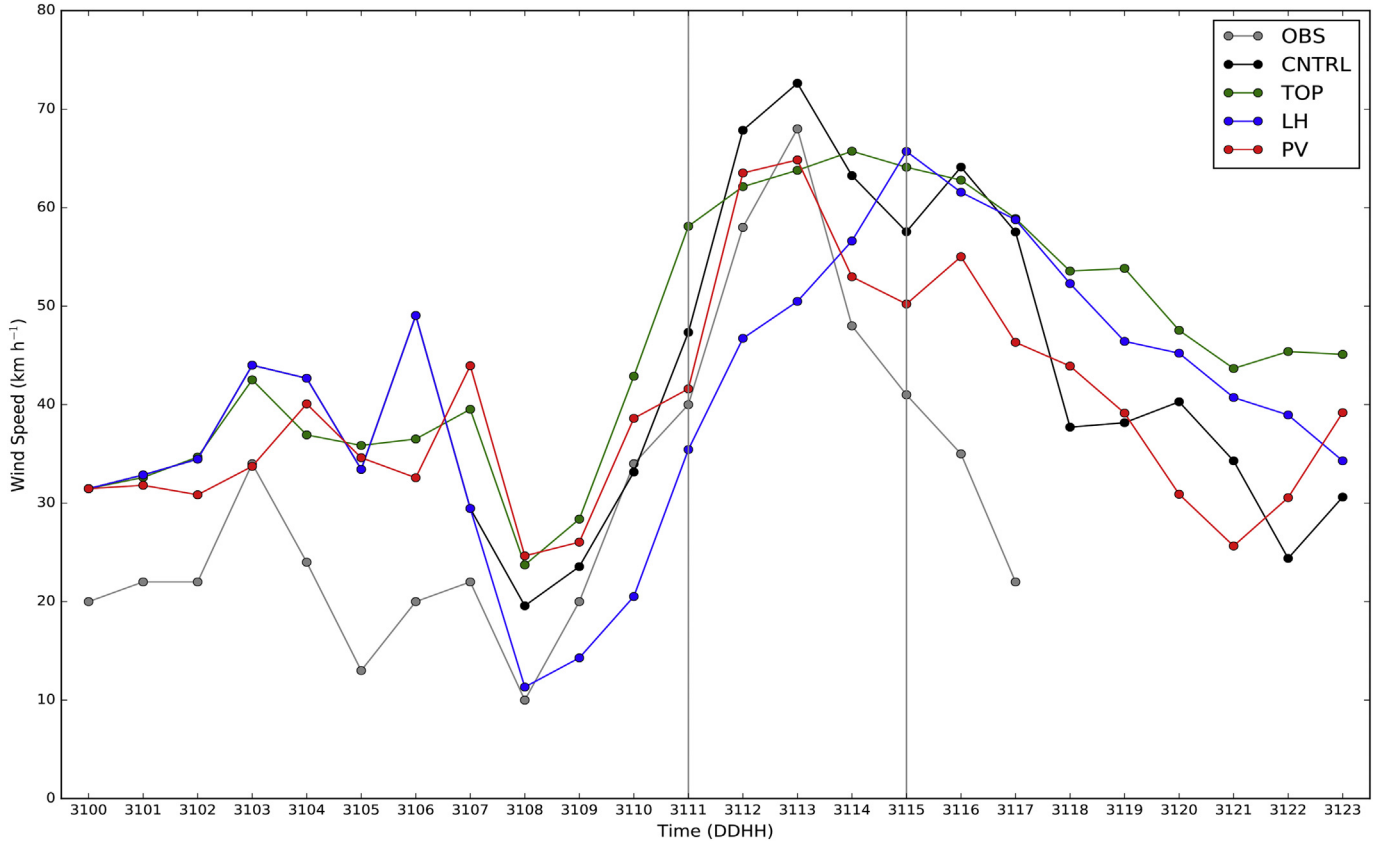

Fig. 7. 10-m wind speed observed (solid grey line) and simulated (solid color lines) by the different numerical experiments performed in this study between 00–23 UTC on 31 October 2012 at the closest point to the airport of Menorca.

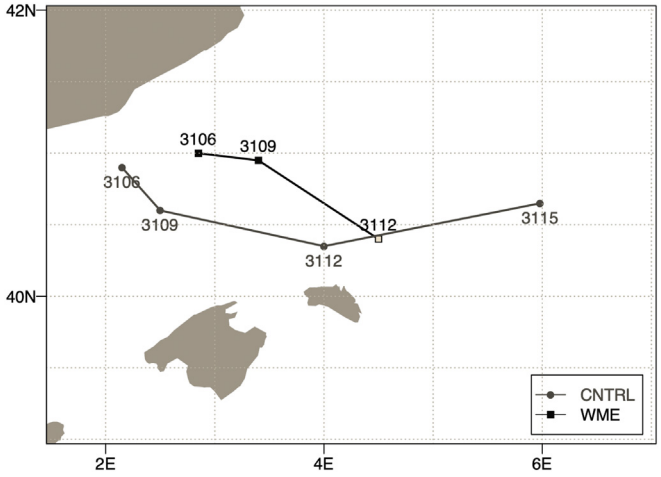

Fig. 8. Track of the secondary cyclone as simulated by the control run (grey solid line) and analysed by in comparison to the AROME-WMED's reanalysis (black solid line) between 06–15 UTC on 31 October 2012.

latent heat release contributed to the small and rapidly developing genesis of the secondary cyclone (Fig. 10 (d-f)). In the following hours, the convergence area intensified and moved south-eastwards, accompanying the secondary cyclone, which continued its deepening, while moving towards Minorca.

The maritime flow responsible of the low-level convergence area was driven by the PC that initiated offshore Murcia, north of the Algerian coast, which is clearly characterized by the control run with a warm and a cold sector (Fig. 11). Taking into account the low-level wind field depicted in Fig. 10 we can infer that the warm and dry air from the warm sector was advected towards a colder and moist air located over the Catalan region, increasing the chances of atmospheric convective instability, and thus strengthening the favourable environmental conditions required to initiate the secondary cyclone. In order to better understand the thermodynamical environment in which the secondary cyclone took place, we analyse the vertical distribution of the equivalent potential temperature and wind fields along the SC trajectory (Fig. 12).

During the first hours of 31 October the warm front of the primary cyclone was located over the sea and penetrated over the colder air located over the Catalan coast, favouring the instability and thus the air lift (Fig. 12b). This potential instability is clearly identified at the approximate location of 41.61° latitude and 2.03° longitude (see dotted lines in Fig. 12a). At 08 UTC, the time SC developed and started its intensification, strong vertical winds were simulated over the Catalan coast (Fig. 12c), advecting warm air to the mid- and upper-levels, thus forming a warm core for SC. In addition, the synoptic environment was also favourable for ascents from strong quasi-geostrophic forcings (see

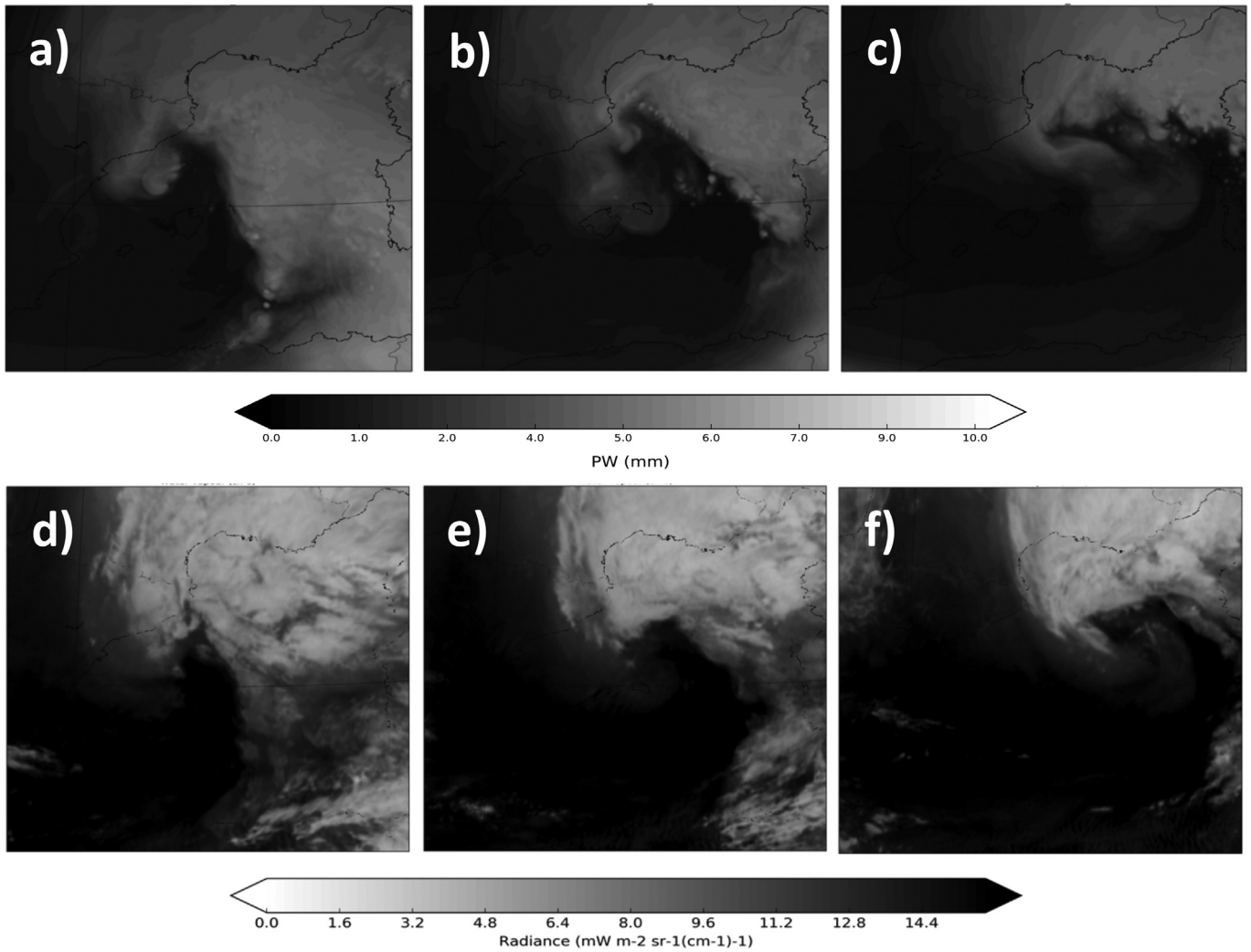

Fig. 9. Simulated precipitable water (mm) integrated over 650–200 hPa layer (a-c) and water vapour radiance (6.2 μm) from METEOSAT-SEVIRI satellite (d-f) at (a,d) 09, (b,e) 12 and (c,f) 15 UTC on 31 October 2012.

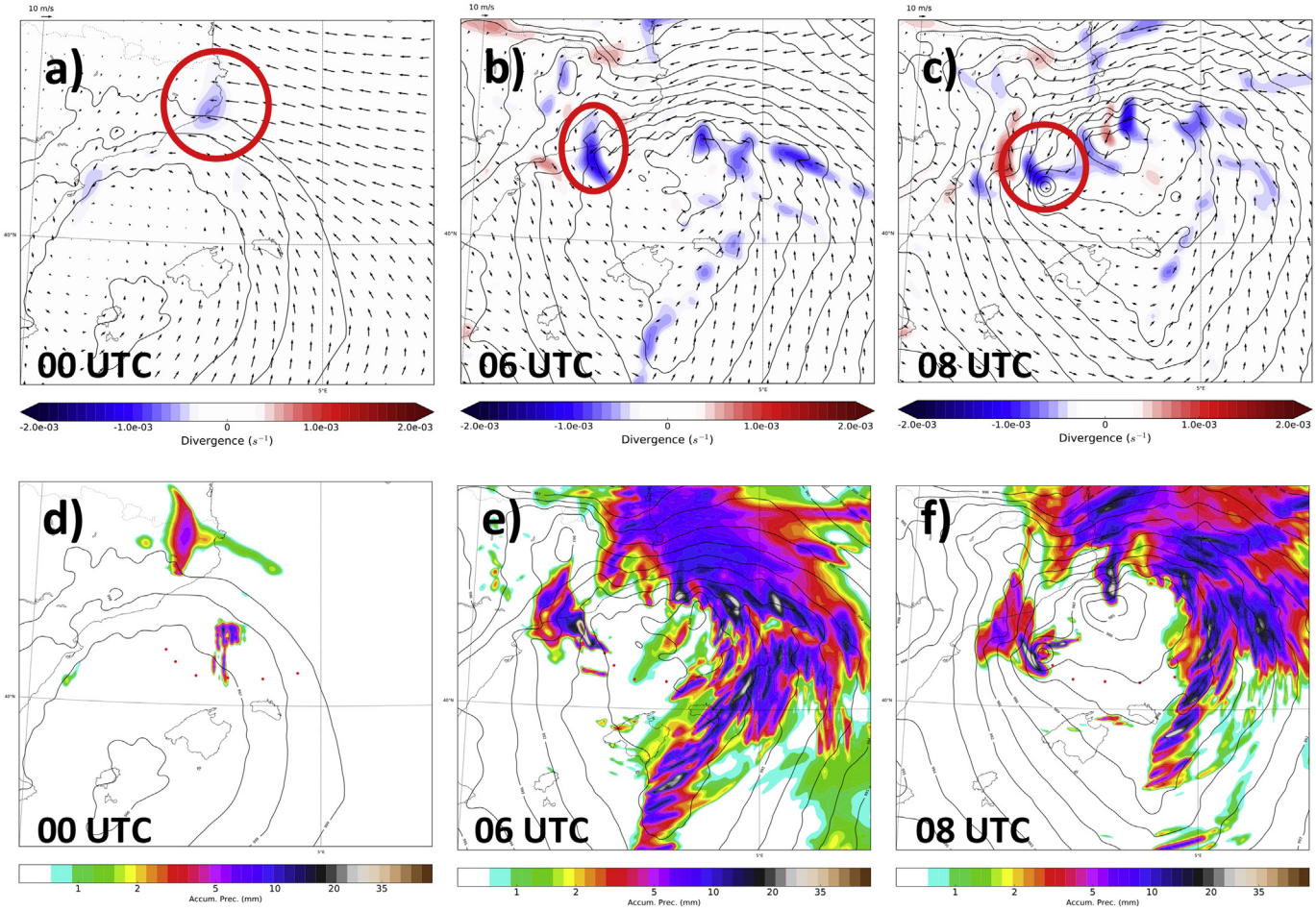

Fig. 10. Control surface divergence, horizontal winds and MSLP (a-c) and hourly accumulated precipitation together with MSLP (d-f) depicted at a-d) 00, b-e) 06 and c-f) 08 UTC on 31 October 2012. Red circle highlights locations of low-level convergence associated with triggering of the secondary cyclone. (For interpretation of the references to colour in this figure legend, the reader is referred to the web version of this article.)

Fig. 7 in Flaounas et al., 2016).

In order to complete the thermodynamical diagnosis of this event, we have also investigated the effect of the surface heat fluxes on the genesis of the SC through the latent and sensible heat flux. During the first hours of 31 October latent heat fluxes show only marginal positive values (Fig. 13a). However, the sensible heat flux showed larger values spread over the north-eastern part of the Balearic Islands (Fig. 13d), associated with the intrusion of the warmer and moist air tongue from northern Africa. At 0800 UTC, the surface latent heat flux shows a significant signal offshore Catalonia (Fig. 13b), over the same region where previously we identified a low-level convergence zone that plays an important role favouring the triggering of deep convection of the SC (Fig. 10). At the same time, the surface sensible heat flux also shows large values over the same region associated with the initiation of the SC. The latent heat flux signature associated to the initiation of the SC evolved in the following hours according to the evolution of the SC and became stronger, reaching its maximum intensity over north-eastern Majorca, and affecting Majorca and Minorca Islands at 1200 UTC (Fig. 13c). Simultaneously, the sensible heat flux reveals a maximum at the same location linked to the SC (Fig. 13f).

5. Sensitivity experiments

In order to confirm the diagnosis analysis of the event described in the previous sections, a set of sensitivity experiments are performed considering three main factors (Table 1). On the one hand, the presence of vorticity advection associated with the intense upper-level trough and the intrusion of dry air suggest that the potential vorticity anomaly (PV) associated with the trough is a determinant factor for the cyclogenesis of the secondary low. On the other hand, the initial stages of SC took place near intense precipitation areas, where latent heat release could have had a relevant role in the development and intensification of the SC. Consequently, latent heat release is also considered in the analysis. Finally, it is noteworthy that the primary low-pressure system advects warm and moist air from the Mediterranean Sea towards the coast of Catalonia. This flow would provide moisture and also progressively build up a convectively unstable layer that, in conjunction with the topographic lift, would enhance the intensity of convection and eventually contribute to the secondary cyclogenesis. In order to test this hypothesis, we also numerically investigate the role of the orography on the formation and evolution of SC.

5.1. Experiments design

In order to assess the impact of the upper-level dynamics on the secondary cyclogenesis, the PV-inversion technique of Davis and Emanuel (1991) is applied. In essence, this technique allows to modify model fields while conserving adequate balances through the invertible principle. In this study, the PV-inversion technique is applied over the 16-km grid resolution parent domain. The 300 hPa PV field clearly shows the intense anomaly signalling the upper levels deep trough (Fig. 14a). The precise design of a sensitivity experiment consisting of removing potential vorticity from the initial fields is delicate. Indeed, removing the entire PV anomaly would produce a drastic change in the

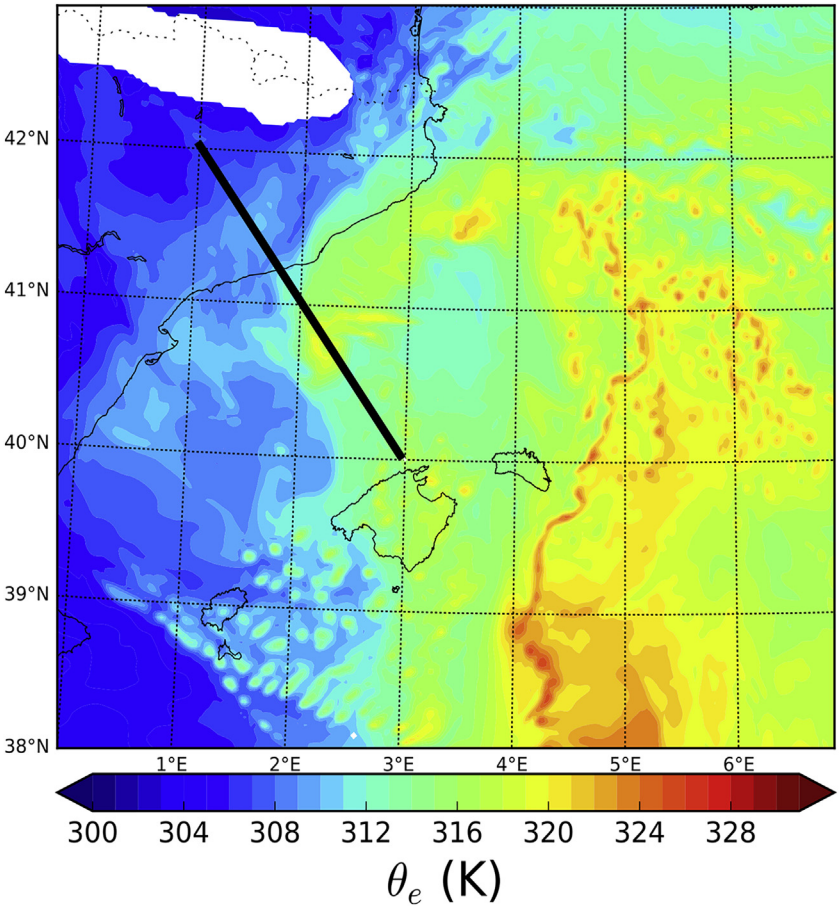

Fig. 11. Control equivalent potential temperature (EPT) at 08 UTC on 31 October 2012. Black line represents the region used to represent a cross-section of the EPT.

evolution and lead to the obvious conclusion that the upper levels forcing is key for the evolution of the PC and the formation of the SC. Instead, we perform a much subtle analysis and focus on the effect of minor modifications to the PV field. In particular, we test the effect of the portion of the PV streamer that was located over the north-eastern part of the Iberian Peninsula (white box in Fig. 14a). Locally reducing the amplitude of PV by 5% results in a weakening of the upper-level trough, removing the isolated cut-off circulation (Fig. 14b). The resulting weakened PV field is inverted, and the modified fields are used to initialize EXP_PV.

With regard to the impact of the diabatic heating produced by latent heat release from condensation, we design a numerical experiment with no latent heat release after 0700 UTC on October 31, 2012 (EXP_LH), which is the initiation time of the secondary cyclone in the control experiment. Turning off this factor at SC genesis time will allow to focus on the effect of diabatic heat fluxes during its life-cycle.

Finally, the hypothesized influence of the orography on the event is also numerically tested. An experiment with the Pyrenees and Balearic Islands lowered to sea level height (EXP_TOP) is intended to evaluate the effects of local topographic lifting and flow modification on the initiation processes and posterior development of the secondary cyclone.

5.2. Experiments results

A notably high difference in the evolution of the MSLP field across experiments is obtained and reveals high sensitivity to the selected factors. First, we pay special attention to the time the secondary cyclone reached its maximum deepening in CTRL, at 1200 UTC on October 31, 2012 (Fig. 15).

EXP_PV shows the sensitivity of the genesis and evolution of the secondary cyclone to small modifications of the upper-level trough via the reduction of a portion of the PV streamer. In fact, the reduction of a minimal portion the PV streamer (5%) already reflects a weaker intensity and also a notable northward displacement of the SC path. Despite producing a weaker SC than the control run, EXP_PV still produces a strong pressure gradient over Minorca, generating similar winds to those observed (Fig. 15). However, the simulated pressure record for the Minorca airport is shallower than for the other numerical experiments (Fig. 6). This numerical experiment has shed light on the notable loss of intensity and track deviation of the secondary cyclone produced by the reduction of a marginal portion of the PV streamer (5%). This reduction of PV has slightly affected low-level dynamics and thermodynamics. In terms of dynamics, the low-level convergence zone remains unchanged with respect to the control experiment. The wind and MSLP fields also remain unaltered. In addition, low-level thermodynamics are neither modified significantly, showing both the warm and cold sectors of the PC, as in the control experiment. However, the reduction of the upper-level dynamics has affected the mesoscale circulation and thermodynamics of the mid- upper- tropospheric levels, reducing the cold air aloft and thus, decreasing the convective instability and, consequently, the depth and intensity of the secondary cyclone.

As expected, EXP_LH does not generate SC, which confirms the primary diabatic character of this secondary system. Taking into account that EXP_LH removes the contribution of latent heat release after 0700 UTC, it also simulates a weakened PC from that moment onwards, which evolves from the Catalan coast to Sardinia, affecting Minorca along its path. In agreement with this, the simulated MSLP at the Minorca airport is higher than observed (Fig. 6). Thus, diabatic latent

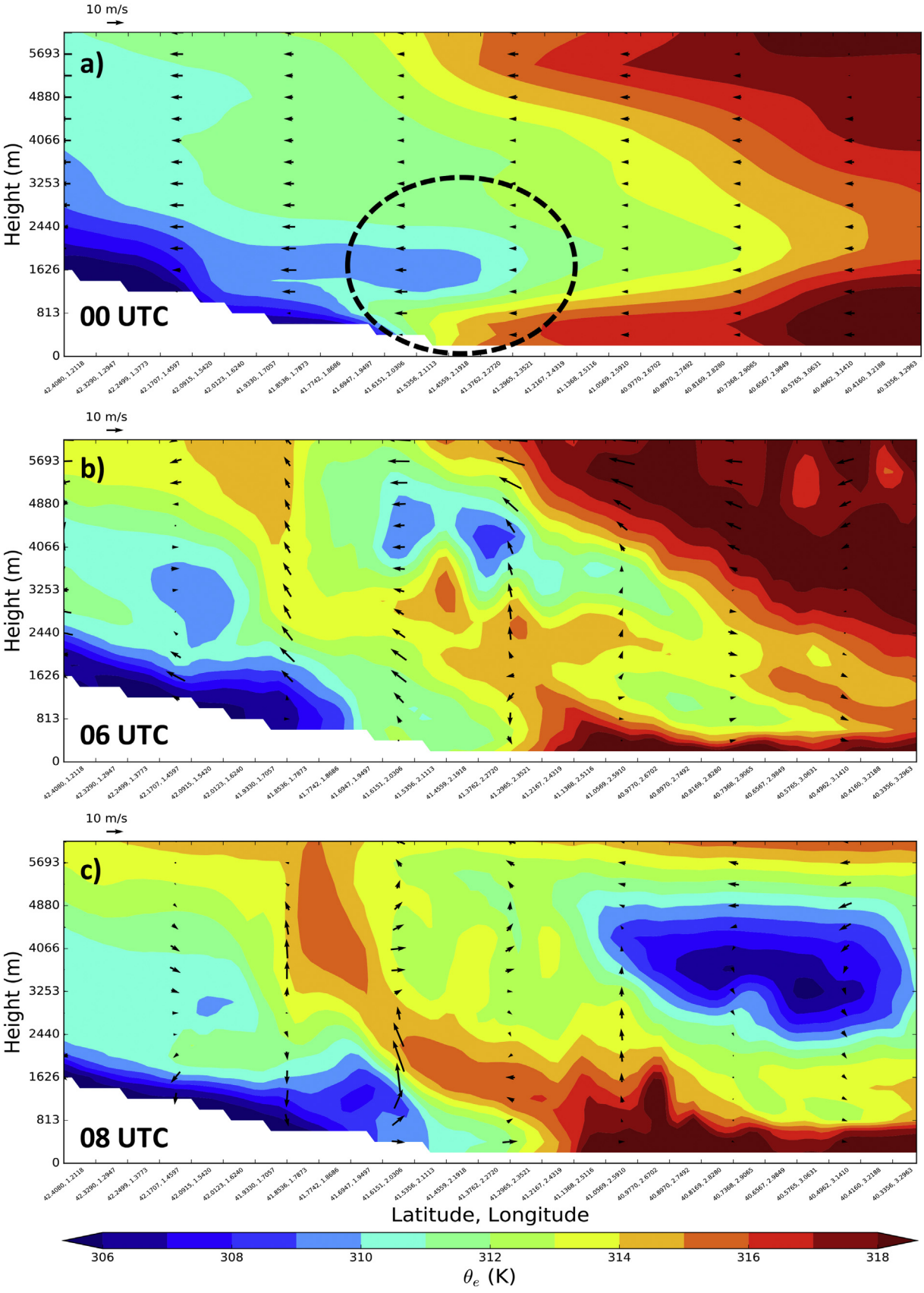

Fig. 12. Cross-section of the equivalent potential temperature (color filled) and wind (black arrows) fields at a) 00 UTC, b) 06 UTC and c) 08 UTC on 31 October 2012. Dotted line in a) indicates potential instability. The georeferenced location of this cross-section is performed in Fig. 11.

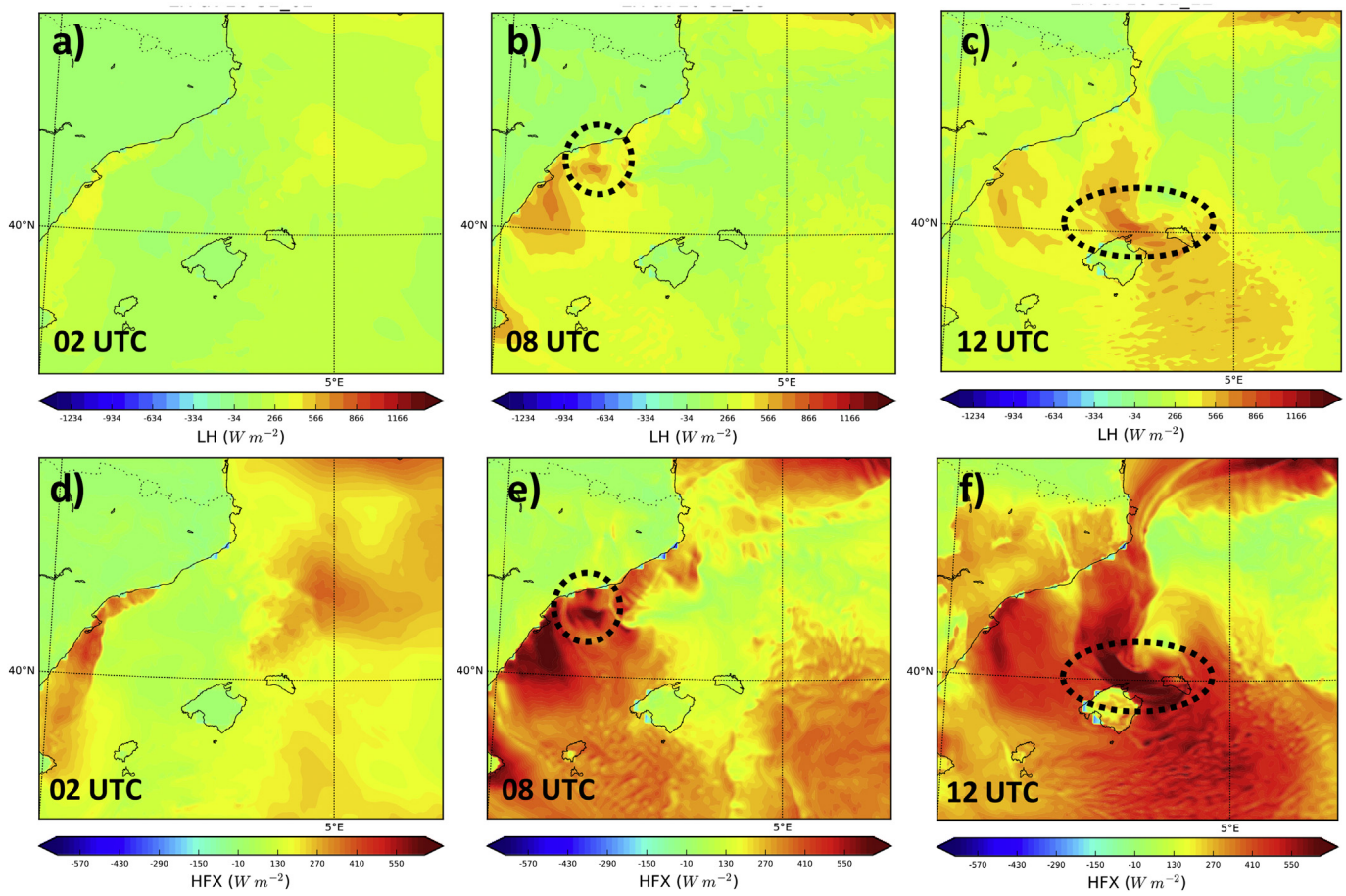

Fig. 13. Surface latent heat flux (a-c) and upward sensible heat flux (d-f) depicted at a-d) 02, b-e) 08 and c-f) 12 UTC on 31 October 2012.

Table 1
Configuration of the sensitivity experiments: 1 indicates the factor is activated during the simulation and 0 otherwise.

Experiment	Latent-heat release	PV anomaly	Topography
EXP_CNTRL	1	1	1
EXP_LH	0	1	1
EXP_PV	1	0	1
EXP_TOP	1	1	0
EXP_LHP	0	1	0
EXP_LHV	0	0	1
EXP_TOV	0	1	1
EXP_REF	0	0	0

heat release plays a determinant role in the genesis of the secondary low.

The EXP_TOP simulation reveals the important role of the local topography in the genesis and posterior evolution of the secondary low, without significant effect on the PC, similarly to EXP_PV. EXP_TOP also produces a strong pressure gradient (Fig. 15) although for a longer period. In addition, the lack of orographic forcing influences the low-level convergence zone originated near the Catalan coast (Fig. 10a), which is the main triggering mechanism for the cyclogenetic convection. As mentioned earlier, this low-level convergence originates from the interaction of the western-southwestern warm and moist air tongue with the topography, that forces the impinging air to lift, favouring the convective initiation and the SC genesis. When such topography is removed, a substantial modification of the PC is obtained and thus the SC is not generated. As a result, the MSLP drop signature in EXP_TOP at the Minorca's airport location (Fig. 6) is linked to the principal cyclone only. This explains the similarities between EXP_TOP and CNTRL in MSLP during the first 7–8 h of simulation (Fig. 6), as the main difference between them is the generation of SC in the control run.

In summary, it is important to highlight that the three considered factors (PV, latent heat release, and topography) play different roles in the cyclogenesis and evolution of the small and intense secondary low-pressure system that affected the island of Minorca on October 312,012, confirming the conceptual model described in the previous sections.

5.3. Factor separation

The factor separation technique (Stein and Alpert, 1993) is a powerful algorithm that allows to quantitatively determine the individual, as well as synergistic effects of a set of predetermined factors on a particular simulated aspect. In order to properly quantify the individual and combined effects of the 3 factors considered here, this technique requires 2^3 simulations (Table 1).

To be able to assess the individual effect of each factor, as well as their synergies, we analyse the time evolution of the MSLP following the trajectory of the secondary low-pressure system centre in the control simulation (Fig. 16). Results show that during the genesis of the secondary cyclone, the reduction of the upper-level PV anomaly and the removal of latent heat fluxes contributed to the cyclogenesis, with the PV contribution being stronger initially. This result confirms the key role of the upper-level PV anomaly acting as a triggering mechanism of air-sea instability (Emanuel, 1986; Romero, 2001; Homar et al., 2002; Romero et al., 2006; Fita et al., 2007b) to the initiation of this SC. After the initial deepening phase, the effect of the reduction of the upper-level PV anomaly on the MSLP is gradually becoming less dominant, while the latent heat release effect remains almost uniform. At this point, individual latent heat release and PV effects on the MSLP become

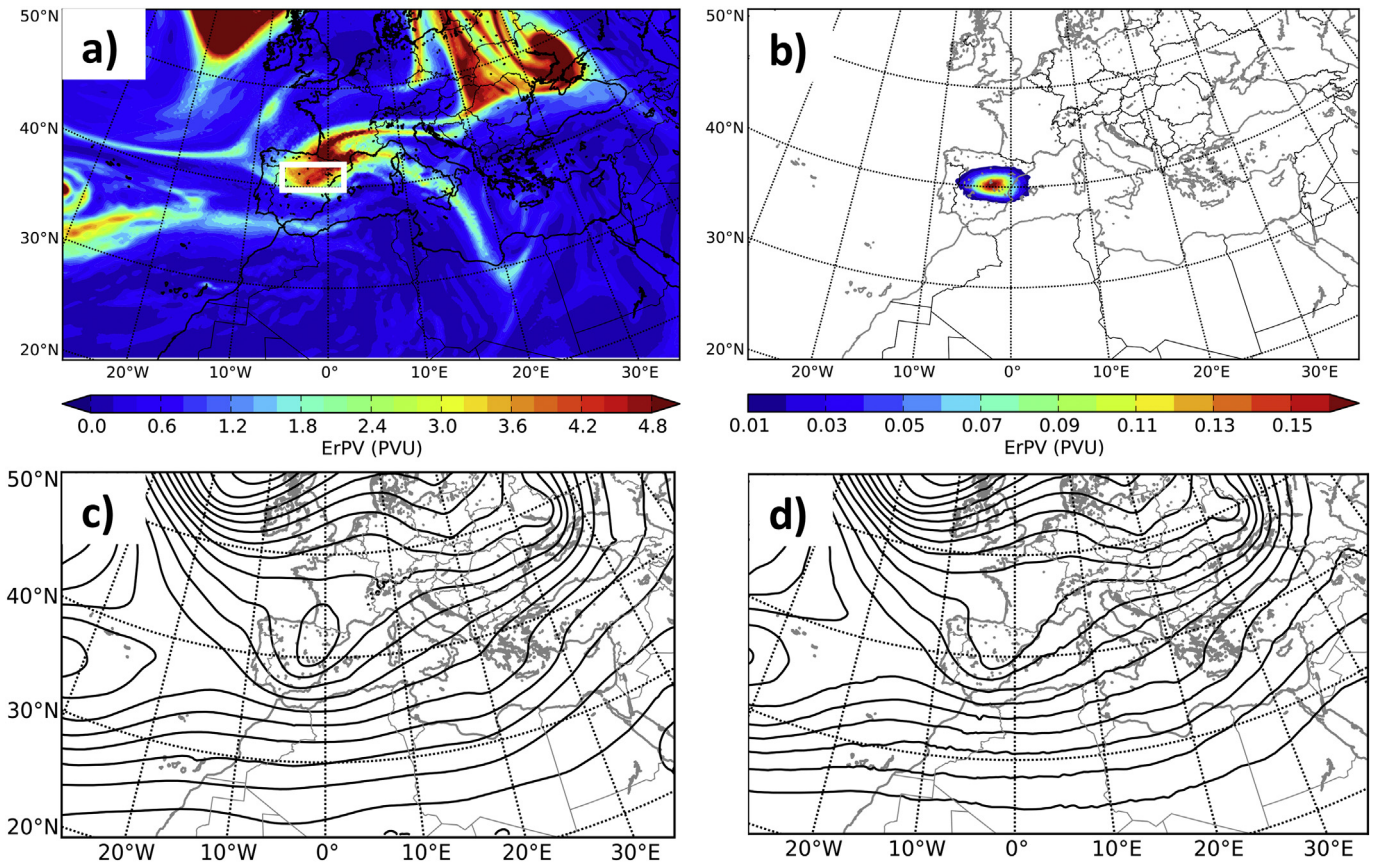

Fig. 14. a) Control potential vorticity (PVU), b) potential vorticity perturbation (PVU) removed from the.
field in panel a) to apply the inversion and obtain the field in panel d). Control (c) and perturbed (d) geopotential height (gpm) at 300 hPa at 00 UTC 31 October 2012. The perturbed field was used as initial conditions for the EXP_PV simulation.

indistinguishable. However, from 1200 UTC, the latent heat release become the most relevant effect maintaining and intensifying the SC until the end of the simulation. Nevertheless, the synergistic effect between PV and topography provides the main factor that dominates the initiation and evolution of the secondary low-pressure system, contributing more than any other effect. The intensity of this combined effect reaches approximately 5 hPa at 0700 UTC and in the following hours reduces to 3–4 hPa. It is important to note that the synergism between different factors should not be interpreted as a simultaneous action, but as a consequence of a collaborative effect, which would not occur without each individual contribution. In this case, the SC is initially forced by specific details of the upper-level dynamics, together with appropriate modifications in the atmospheric flow produced by prominent topography, which lead to the genesis and evolution of the SC. Interestingly, topography is the only factor that individually contributed cyclolytically on the SC. This result is a local consequence of the modification of the low levels flow by the orography, which produces a location and intensity modification to the SC.

6. Conclusions

During the HyMeX-SOP1 campaign, on 31 of October 2012 (IOP18) heavy rain and strong winds (72 km/h sustained speed, with gusts of 117 km/h) affected the island of Minorca. This high-impact event was associated with a secondary cyclone (SC) that formed and intensified within a prominent Mediterranean cyclone (PC). The secondary cyclone formed offshore the Catalonian coast, where heavy rain was observed, and then evolved towards the south-east, reaching Minorca. Heavy precipitation –hypothetically related with the formation of the secondary cyclone - was registered in Catalonia (112 mm in 12 h) and in Majorca (60 mm in 12 h). The present work aims, on the one hand, to document and diagnose aspects of the IOP18 event, and on the other hand, to understand, through high-resolution numerical simulations, the physical mechanisms that contributed to the formation of the secondary cyclone that affected Minorca Island.

A description of the IOP18 synoptic and mesoscale settings was conducted using the AROME-WMED reanalysis. Due to its fine grid resolution and the fact that it assimilates information from different observations, the AROME-WMED was able to identify not only the evolution of the main cyclone, but also the small-scale substructure initiated over the Catalan coast several hours later. A cyclone tracking algorithm was applied, as a useful tool to identify and follow the main cyclone as well as the secondary cyclone. This SC was small in size and intense in terms of geostrophic vorticity. At 1200 UTC, the SC was located north of Minorca and produced the strong westerly winds registered in the Minorca airport.

In order to investigate the physical mechanisms behind the genesis and posterior evolution of the SC, high-resolution numerical simulations using the WRF mesoscale model are performed. We found that the main cyclogenetic mechanism of this SC during the initial stages was related with the latent heat release from heavy precipitation offshore the Catalan coast. The moist convection was triggered over a low-level convergence area primary originated by the intrusion of warm and moist air impinging the Catalan coast. Schematically, during the formation and life-cycle of this SC, three main factors were present. On the one hand, a strong upper-level vorticity advection forcing, associated with the presence of an intense upper-level trough is detected over the SC area. Then, the diabatic heating from condensation in the heavy precipitation area could play an important role. And finally, the complex topography over the Iberian Peninsula and the Balearic Islands

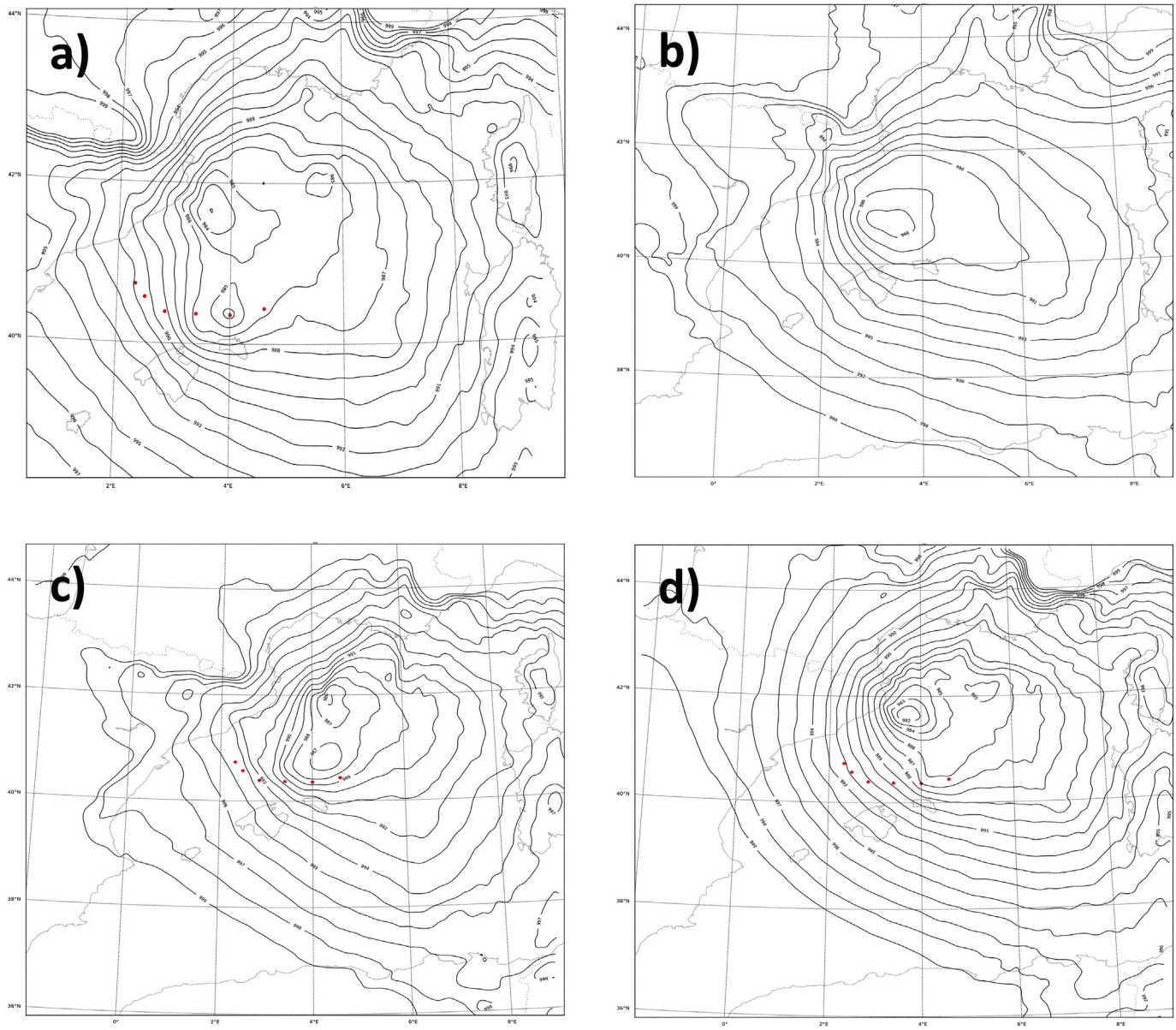

Fig. 15. MSLP (hPa, solid line) and secondary cyclone track (red dots) at 12 UTC 31 October 2012 for a) CNTRL, b) EXP_LH, c) EXP_PV and d) EXP_TOP. (For interpretation of the references to colour in this figure legend, the reader is referred to the web version of this article.)

could have contributed to lift moist and warm air, favouring vertical motion and the triggering of deep convection. With the main objective of quantifying the role of these three factors (i.e., PV, latent heat release and topography), we performed a set of numerical sensitivity experiments. Results confirm the influence of these three factors, highlighting the role of the latent heat release and topography over specificities of the upper-level forcing.

To be able to quantitatively determine the individual and the synergistic effects of these three factors, we have applied the factor separation technique. Results show that both PV and latent heat release individual effects contribute significantly to the secondary cyclone formation. In particular, the PV anomaly effect dominates during the first stage of the initiation of this SC and then, during the following hours, the latent heat release effect became as important as the PV effect. Interestingly, the PV effect remains almost uniform along the entire numerical simulation. From 11 UTC to the end of the simulation period, it is noticed a strong negative tendency on the MSLP due to the latent heat release effect, likely related with the mature phase of the SC and the precipitation associated to it. Regarding synergies, it was observed that the combined effect of the PV anomaly and the topography factors was the most relevant one favouring the SC formation and intensification, along its entire life cycle. However, if we consider the synergism of the three factors, the effect on the MSLP reduces significantly, as we could infer from the pressure rising effect related with the latent heat release. For these reasons, we conclude that the synergy between topography and PV played the leading role in the intensification and evolution of the secondary low-pressure centre that affected Minorca, followed by the triple synergy between the three factors.

Finally, from the point of view of improving the numerical predictability of small-scale intense weather events, especially those originated over the sea, this paper also highlights the great importance of understanding, identifying and capturing all the main physical factors involved in the genesis and evolution of such events.

Acknowledgements

This research is framed within the CGL2017-82868-R [Severe

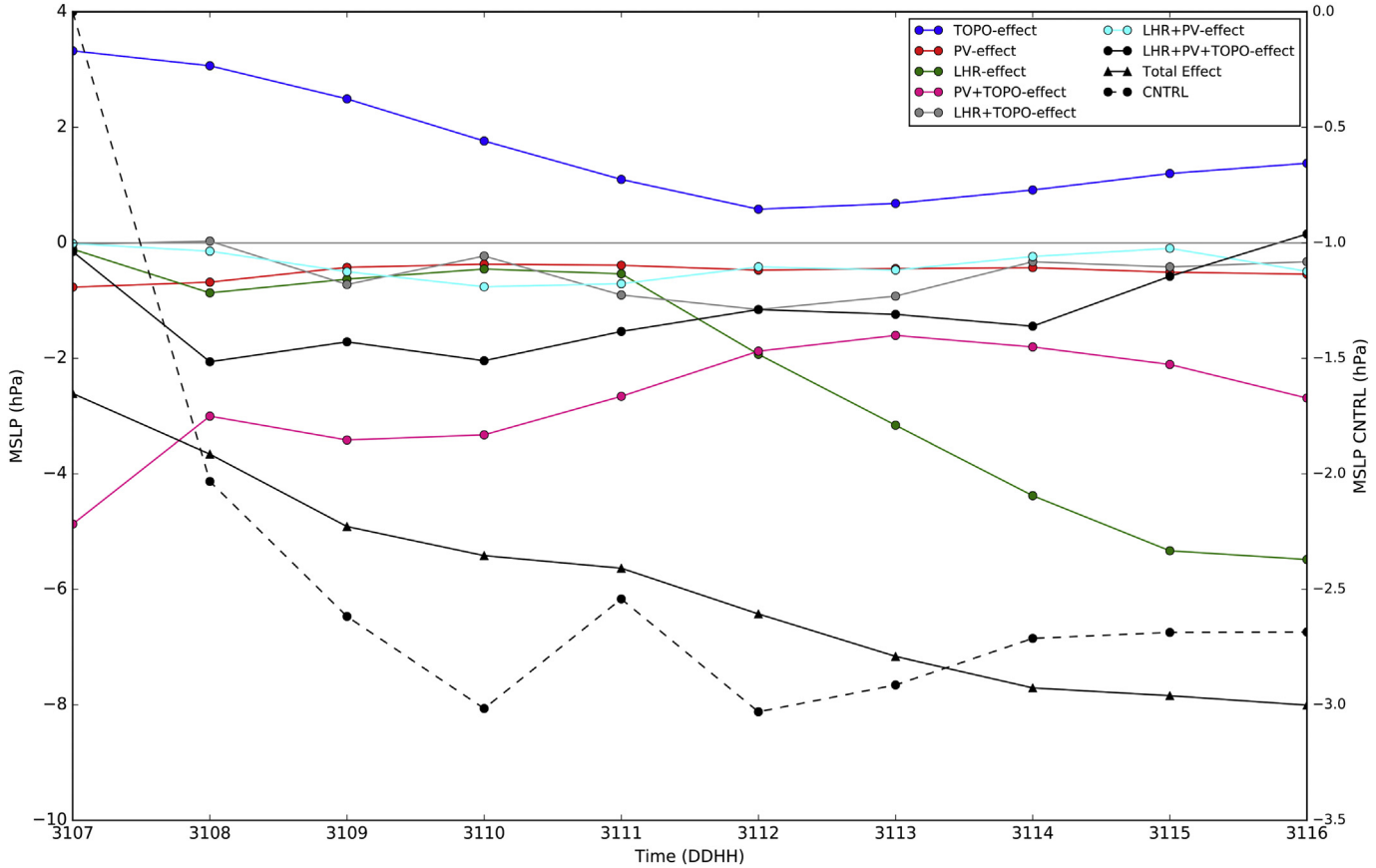

Fig. 16. Representation of all the individual and synergism effects over the MSLP drop, spatially averaged (10 x 10 km2) around the secondary cyclone center, during 31 October2012. Total effect is also shown (see legend). Refere.

Weather Phenomena in Coastal Regions: Predictability Challenges and Climatic Analysis (COASTEPS)] Spanish project which is partially supported with AEI/FEDER/MINECO funds.

Declaration of Competing Interest

The authors declare that they have no known competing financial interests or personal relationships that could have appeared to influence the work reported in this paper.

References

Buzzi, A., 2010. Synoptic-scale variability in the Mediterranean. In: ECMWF Seminar on Predictability in the European and Atlantic regions, 6–9 September. vol. 2010. pp. 15–29.

Campins, J., Jansà, A., Genovés, A., 2006. Three-dimensional structure of western Mediterranean cyclones. Int. J. Climatol. 26 (3), 323–343.

Carrió, D.S., Homar, V., Jansà, A., Romero, R., Picornell, M.A., 2017. Tropicalization process of the 7 November 2014 Mediterranean cyclone: numerical sensitivity study. Atmos. Res. 197, 300–312.

Davis, C.A., Emanuel, K.A., 1991. Potential vorticity diagnostics of cyclogenesis. Mon. Weather Rev. 119 (8), 1929–1953.

Davolio, S., Miglietta, M.M., Moscatello, A., Pacifico, F., Buzzi, A., Rotunno, R., 2009. Numerical forecast and analysis of a tropical-like cyclone in the Ionian Sea. Nat. Hazards Earth Syst. Sci. 9 (2), 551–562. https://doi.org/10.5194/nhess-9-551-2009.

Drobinski, P., Ducrocq, V., Alpert, P., Anagnostou, E., Béranger, K., Borga, M., Braud, I., Chanzy, A., Davolio, S., Delrieu, G., Estournel, C., Boubrahmi, N.Filali, Font, J., Grubiši'c, V., Gualdi, S., Homar, V., Ivan˘can-Picek, B., Kottmeier, C., Kotroni, V., Lagouvardos, K., Lionello, P., Llasat, M.C., Ludwig, W., Lutoff, C., Mariotti, A., Richard, E., Romero, R., Rotunno, R., Roussot, O., Ruin, I., Somot, S., Taupier-Letage, I., Tintore, J., Uijlenhoet, R., Wernli, H., 2014. HyMeX: A 10-Year Multidisciplinary Program on the Mediterranean Water Cycle. Bull. Amer. Meteor. Soc. 1063–1082 (2014), 95. https://doi.org/10.1175/BAMS-D-12-00242.1.

Ducrocq, V., Braud, I., Davolio, S., Ferretti, R., Flamant, C., Jansa, A., Kalthoff, N., Richard, E., Taupier-Letage, I., Ayral, P.A., Belamari, S., Berne, A., Borga, M., Boudevillain, B., Bock, O., Boichard, J.L., Bouin, M.-N., Bousquet, O., Bouvier, C., Chiggiato, J., Cimini, D., Corsmeier, U., Coppola, L., Cocquerez, P., Defer, E., Drobinski, P., Dufournet, Y., Fourrié, N., Gourley, J.J., Labatut, L., Lambert, D., Le Coz, J., Marzano, F.S., Molinieì, G., Montani, A., Nord, G., Nuret, M., Ramage, K., Rison, B., Roussot, O., Said, F., Schwarzenboeck, A., Testor, P., Van Baelen, J., Vincendon, B., Aran, M., Tamayo, J., 2014. HyMeX-SOP1, the field campaign dedicated to heavy precipitation and flash flooding in the northwestern Mediterranean. Bull. Am. Meteorol. Soc. https://doi.org/10.1175/BAMS-D-12-00244.1. (online first).

Emanuel, K.A., 1986. An air-sea interaction theory for tropical cyclones. part i: Steady-state maintenance. J. Atmos. Sci. 43, 585–604.

Emanuel, K.A., 2005. Genesis and maintenance of “Mediterranean hurricanes”. Adv. Geosci. 2, 217–220. https://doi.org/10.5194/adgeo-2-217-2005.

Fita, L., Romero, R., Luque, A., Emanuel, K., Ramis, C., 2007a. Analysis of the environments of seven Mediterranean tropical-like storms using an axisymmetric, non-hydrostatic, cloud resolving model. Nat. Hazards Earth Syst. Sci. 7, 41–56.

Fita, L., Romero, R., Ramis, C., 2007b. Objective quantification of perturbations produced with a piecewise PV inversion technique. Annales Geophysicae, European Geosciences Union 25 (11), 2335–2349.

Processes leading to heavy precipitation associated with two Mediterranean cyclones observed during the HyMeX SOP1. Flaounas, E., Lagouvardos, K., Kotroni, V., Claud, C., Delanoë, J., Flamant, C., Madonna, E., Wernli, H. (Eds.), Q.J.R. Meteorol. Soc. 142, 275–286. https://doi.org/10.1002/qj.2618.

Fourrié, N., and Nuret, M., 2014: Reanalysis_AROME_WMED_V1. doi: https://doi.org/10.6096/HYMEX.REANALYSIS_AROME_WMED_V1.2014.02.10.

Homar, V., Romero, R., Ramis, C., Alonso, S., 2002. Numerical study of the October 2000 torrential precipitation event over eastern Spain: analysis of the synoptic-scale stationarity. Ann. Geophys. 20, 2047–2066. https://doi.org/10.5194/angeo-20-2047-2002.

Homar, V., Romero, R., Stensrud, D.J., Ramis, C., Alonso, S., 2003. Numerical diagnosis of a small, quasi-tropical cyclone over the western Mediterranean: dynamical vs. boundary factors. Q. J. R. Meteorol. Soc. 129, 1469–1490. https://doi.org/10.1256/qj.01.91.

Hong, S.Y., Noh, Y., Dudhia, J., 2006. A new vertical diffusion package with an explicit treatment of entrainment processes. Mon. Weather Rev. 134 (9), 2318–2341.

Iacono, M.J., Delamere, J.S., Mlawer, E.J., Shephard, M.W., Clough, S.A., Collins, W.D., 2008. Radiative forcing by long-lived greenhouse gases: calculations with the AER radiative transfer models. J. Geophys. Res. Atmos. 113 (D13).

Jansà, A., Campins, J., Picornell, M.A., Guijarro, J.A., 2014. Heavy rain and strong wind

events over Spain during HyMeX SOP1. (Tethys).
Kain, J.S., 2004. The Kain–Fritsch convective parameterization: an update. J. Appl. Meteorol. 43 (1), 170–181.
Kain, J.S., Fritsch, J.M., 1993. Convective parameterization for mesoscale models: The Kain- Fritsch scheme. In: The representation of cumulus convection in numerical models. American Meteorological Society, Boston, MA, pp. 165–170.
Lagouvardos, K., Kotroni, V., Nickovic, S., Jovic, D., Kallos, G., Tremback, C.J., 1999. Observations and model simulations of a winter sub-synoptic vortex over the central Mediterranean. Meteorol. Appl. 6, 371–383. https://doi.org/10.1017/S1350482799001309.
Mariani, S., Casaioli, M., Malguzzi, P., 2015. Towards a new BOLAM-MOLOCH suite for the SIMM forecasting system: implementation of an optimised configuration for the HyMeX Special Observation Periods. Nat. Hazards Earth Syst. Sci. Discuss. 2, 649–680. https://doi.org/10.5194/nhessd-2-649-2014.
Neu, U., Akperov, M.G., Bellenbaum, N., Benestad, R., Blender, R., Caballero, R., ... Grieger, J., 2013. IMILAST: A community effort to intercompare extratropical cyclone detection and tracking algorithms. Bulletin of the. vol. 94(4). American Meteorological Society, pp. 529–547.
Picornell, M.A., Jansà, A., Genovés, A., Campins, J., 2001. Automated database of mesocyclones from the HIRLAM(INM) 0.5 analyses in the Western Mediterranean. Int. J. Climatol. 21, 335–354.
Picornell, M.A., Campins, J., Jansà, A., 2013. Detection and thermal description of medicanes from numerical simulation. Natural Hazards and 25, 7417–7447.
Pytharoulis, I., 2018. Analysis of a Mediterranean tropical-like cyclone and its sensitivity to thesea surface temperatures. Atmos. Res. 208, 167–179. https://doi.org/10.1016/j.atmosres.2017.08.009.
Romero, R., 2001. Sensitivity of a heavy-rain-producing western Mediterranean cyclone to embedded potential-vorticity anomalies. Q. J. R. Meteorol. Soc. 127 (578), 2559–2597.
Romero, R., Martín, A., Homar, V., Alonso, S., Ramis, C., 2006. Predictability of prototype flash flood events in the Western Mediterranean under uncertainties of the precursor upper- level disturbance.
Sanders, F., Gyakum, J.R., 1980. Synoptic-dynamic climatology of the “bomb”. Mon. Weather Rev. 108 (10) 1589–160.
Skamarock, W.C., Klemp, J.B., Gill, D.O., Barker, D.M., Wang, W., Powers, J.G., 2008. A description of the advanced research WRF version 3. In: NCAR. Tech. Rep. TN-4751STR. NCAR, Boulder, Colorado, USA (113 pp.).
Stein, U., Alpert, P., 1993. Factor separation in numerical simulations. J. Atmos. Sci. 50 (14).
Thompson, G., Rasmussen, R.M., Manning, K., 2004. Explicit forecasts of winter precipitation using an improved bulk microphysics scheme. Part I: description and sensitivity analysis. Mon. Weather Rev. 132 (2), 519–542.
Thompson, G., Field, P.R., Rasmussen, R.M., Hall, W.D., 2008. Explicit forecasts of winter precipitation using an improved bulk microphysics scheme. Part II: Implementation of a new snow parameterization. Mon. Weather Rev. 136 (12), 5095–5115.
Tous, M., Romero, R., 2013. Meteorological environments associated with medicane development. Int. J. Climatol. 33, 1–14. https://doi.org/10.1002/joc.3428.